AAPS PharmSciTech, Vol. 9, No. 2, June 2008 (© 2008)
DOI: 10.1208/s12249-008-9074-4

Research Article

Pore Direction in Relation to Anisotropy of Mechanical Strength in a Cubic Starch Compact

Yu San Wu,[1,5,6] Lucas J. van Vliet,[2] Henderik W. Frijlink,[1] Ietse Stokroos,[3] and Kees van der Voort Maarschalk[1,4]

Received 3 November 2007; accepted 20 February 2008; published online 9 April 2008

Abstract. The purpose of this research was to evaluate the relation between preferential direction of pores and mechanical strength of cubic starch compacts. The preferential pore direction was quantified in SEM images of cross sections of starch compacts using a previously described algorithm for determination of the quotient of transitions (Q). This parameter and the mechanical strength were evaluated in compacts of different porosities. Starch was chosen as a model compound for materials with ductile behaviour of which tablets with low porosities can be made and which shows some elastic recovery after compaction. At medium and high porosity Q was significantly higher in the images providing a side view of the compact than in the images providing a top view (0.973 vs. 0.927 and 0.958 vs. 0.874 at 0 mm from the side of the compact and 0.956 vs. 0.854 and 0.951 *vs.* 0.862 at 3.5 mm), indicating that the pores were mainly oriented in the direction perpendicular to the direction of compression. This was accompanied by a lower crushing force in this direction. This could be explained by considering the pores as cracks which propagate through the sample during crushing. For both directions the crushing force decreased with increasing porosity. The yield strength of the compacts also decreased with increasing porosity, but this parameter was not dependent on the direction of crushing when the porosity was below 10%. The results show that pore direction significantly influences the crushing force but does not influence the yield strength, at porosities below 10%.

KEY WORDS: anisotropy; compact; fracture; mechanical strength; pore direction.

INTRODUCTION

It is well known that porosity influences the mechanical strength of compacts (1–6) and that the mechanical strength of tablets compressed with uni-axial compression is an anisotropic property, i.e. the mechanical strength depends on the direction of measurement (7–17). In earlier research Ando *et al* (9) and Galen and Zavaliangos (16) determined the mechanical strength and took SEM images of cross sections of the tablets. There was no parameter to quantify the directions of the pores; the human observer determined the orientation of the pores and particles. This suggested that the (anisotropy in) pore structure is the cause of the anisotropy in mechanical strength. In the present paper attention will be paid to both the quantification of the preferential pore direction and the anisotropy in mechanical strength in a cubic starch compact to better understand the correlation between these two parameters. Starch was chosen as a model compound for materials with ductile behavior of which tablets with extremely low porosities can be made and which show some elastic recovery after compaction. It was believed that studying the fracture behavior of compacts with an extremely low porosity would make it easier to evaluate the influence of the pore structure.

MATERIALS AND METHODS

Materials

To obtain bodies with a low porosity we chose to use pregelatinized starch, a visco-elastic material. By using a slow compression rate, a slow decompression rate, and a powder with a relatively high moisture content the powder shows plastic deformation with little relaxation. The 106–150 μm fraction of pregelatinized potato starch (Prejel JF, Avebe, Foxhol, The Netherlands) was obtained by 30 min. vibratory sieving (Fritsch analysette 3, Germany) followed by 12 min air jet sieving over a sieve of 106 μm (Alpine A200, Augsburg, Germany), to remove the fines. Before use the powder was stored at least three days at a relative humidity of

[1] Department of Pharmaceutical Technology and Biopharmacy, University of Groningen, Groningen, The Netherlands.
[2] Quantitative Imaging Group, Department of Imaging Science & Technology, Faculty of Applied Sciences, Delft University of Technology, Delft, The Netherlands.
[3] Laboratory for Cell Biology and Electron Microscopy, University of Groningen, Groningen, The Netherlands.
[4] Department of Pharmaceutics, NV Organon, part of Schering-Plough, Oss, The Netherlands.
[5] Solvay Pharmaceuticals, Building WNH, C.J. van Houtenlaan 36, 1381 CP Weesp, The Netherlands.
[6] To whom correspondence should be addressed. (e-mail: Yu-San.Wu@solvay.com)

70%. The apparent particle density was measured with helium pycnometry (Quantachrome, Syosset, New York, USA). Corrected for the moisture content at a relative humidity of 70%, measured with a moisture analyzer (Sartorius MA40, Göttingen, Germany), this was found to be 1439 kg/m^3.

Tablet Compaction

A hydraulic press (ESH compaction apparatus, Hydro Mooi, Appingedam, The Netherlands) was used to compress the starch in a square shaped die with sides of 7 mm. Before compaction, the die was lubricated with magnesium stearate using a brush. Varying quantities of powder were used to obtain cubic shaped compacts with different porosities. The rate of compression was 0.1 kN/s and the rate of decompression varied between 0.001 kN/s for the compacts with low porosity and 0.1 kN/s for the compacts with higher porosities. Compact thickness was measured immediately after compression, further all compact dimensions were measured after 24 h with an electronic micrometer (Mitutoyo, Tokyo, Japan) and the weight of the compacts was measured with an analytical balance (Mettler-Toledo, Greifensee, Switzerland). The porosity of the compacts was calculated from these data and the true density. The porosity calculated in this way will be referred to as 'porosity' while the porosity calculated with image analysis will be referred to as 'local porosity'.

Determination of Mechanical Properties

For the assessment of the mechanical strength a cubic compact was used. The cubic shape makes it possible to compare the properties in the horizontal direction with the properties in the vertical direction, since the outside dimensions of the compact are the same in all directions. The consequence of this methodology is that the tensile strength of the specimen can not be measured, as is done when a cylindrical body is subjected to the diametric compression test (18). However, if the fracture shows ductile behaviour (i.e. the fracture has been preceded by considerable plastic deformation (19)), it does provide an opportunity to measure the yield strength, which can also be used to describe the mechanical strength.

The mechanical properties of the cubes were determined by compressing these between the punches of a compaction simulator (ESH, Brierley Hill, UK) while registering the force–displacement curve on an X–Y recorder (Kipp & Zonen, Delft, The Netherlands). The upper punch moved downwards with a linear speed of 0.75 mm/s. The strength in the *x*-direction was determined by placing the cube between the upper punch and the lower punch in such a way that the direction of the original compression was perpendicular to the direction of crushing. The strength in the *z*-direction was determined by placing the compact in such a way that the direction of the compression was parallel to the direction of crushing. In this way the force at which fracture occurred (crushing force) was registered. The yield point was defined as the maximum in the stress–strain curve or as the intersection of the two tangents of the initial and final parts of the stress strain curve (20). By dividing the force at which yielding occurred by the area of a side of the cube (49 mm^2) the yield strength was calculated.

Imaging of Planes in the Compact

Compacts were embedded with glycolmethacrylate resin. After hardening of the resin, several planes in the compact were smoothed using a microtome as described earlier (21). The planes in the compact that have been imaged are depicted in Fig. 1. Two sets of images were defined, plan and elevation images. Plan images provide a top view and elevation images provide a side view. Of each plane nine images were taken. Figure 1 also clarifies the nomenclature of the different directions. The *z*-direction is the direction of compression and the *x*- and *y*-direction lie perpendicular to this direction.

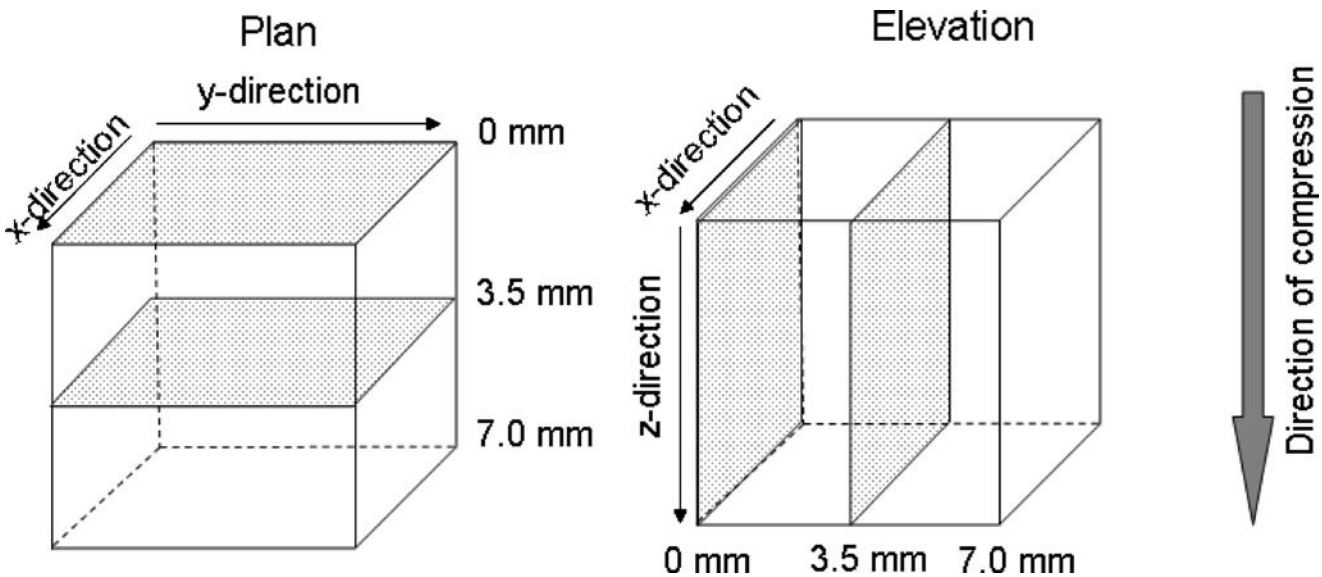

Fig. 1. The locations of the plan images (*left*) and of the elevation images (*right*) in the cubic compact. Per plane nine images were taken in a 3×3 pattern

SEM BEI (Backscattered Electron Imaging) images were taken using a JEOL scanning electron microscope (JEOL, type JSM-6301F with standard paired semiconductor element detector, Japan) operated at an accelerating voltage of 10 kV. The diaphragm was 50 μm and the working distance was 15 mm. The magnification was 60×. Before taking SEM images, the compacts were stored overnight in a closed container with a few osmium tetroxide crystals for evaporation to obtain a better contrast between the resin and the starch in the images.

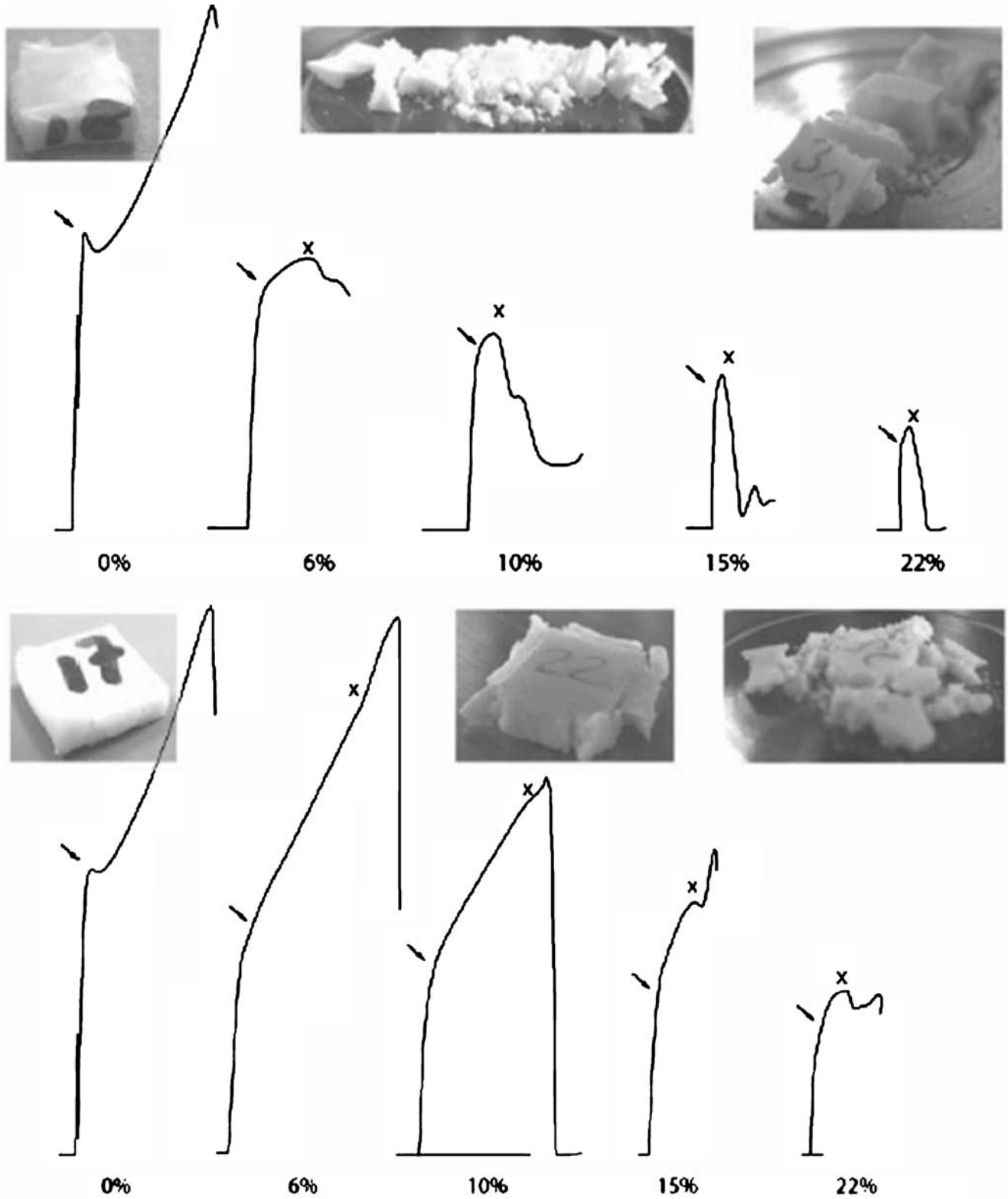

Fig. 2. Force displacement curves of crushing in the *x*-direction (*above*) and in the *z*-direction (*below*) of cubes with a different porosity. *Arrows* indicate yield points and the '*x*' indicates where fracture occurred. The images depict cubes after crushing

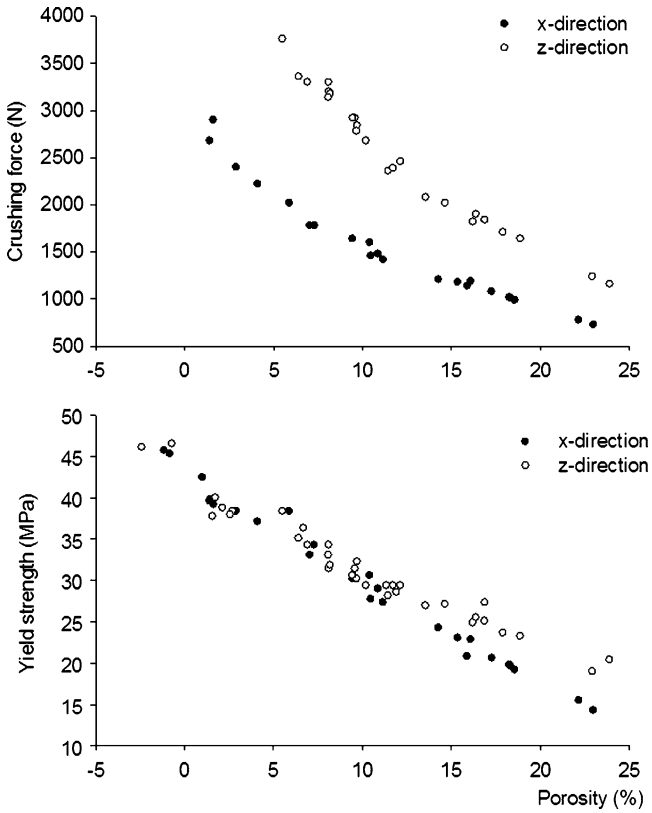

Fig. 3. Crushing force *versus* porosity (*above*) and yield strength *versus* porosity (*below*), in the *x*-direction and the *z*-direction. The porosity was calculated out of weight and volume

Image Analysis

Matlab 7.0.232 R2006a (The MathWorks Inc, Natick, USA) and the DIPimage toolbox version 1.5.3 (Quantitative Imaging Group, Faculty of Applies Sciences, Delft University of Technology, The Netherlands) (22) were used for the image analysis. A previously described method was used to detect a preferential pore direction (21). This method was applied to a cubic NaCl compact with a high porosity. In the present paper we modified this technique to make it suitable for the analysis of starch compacts with low porosities.

The first step in image analysis was the removal of small irregularities in the starch grains so that the borders between the grains and the pores would be clearly defined, while small artefacts caused by the use of the microtome were removed. This was done by using a separable bilateral filter (23). The bilateral filter replaces each pixel value by a weighted sum of its neighbours. The weighting depends on the product of a proximity measure in space (x, y distance) and intensity (pixel value). Both proximities use a Gaussian weighting that decay from the current pixel. The scales (standard deviations) of the two Gaussians were set to respectively 3 pixels and 0.7 times the full-width at half its maximum (FWHM) of the distribution of the pixel values. The FWHM was measured in the grey-value histogram of the image. The histogram shows one great Gaussian shaped peak, with tails to the left and right representing respectively the dark (empty) and white (filled) pore space. The tails have no effect on the measured peak width. The filter's spatial scale is set just large enough to cover the scratches and the intensity scale is set such to encompass noise and scratches in the grains, but to exclude pixel values from across the grain boundary. Hence, the noise is suppressed, but the transitions between grain and pores are preserved (unaltered).

Secondly, the local porosity of the images was determined by counting the white pixels and the black pixels. The segmentation relies on the histogram of the bilateral filtered image. We again measured the position of the peak and its FWHM. We then labelled all pixels that were respectively lower or higher than 1.25 times the FWHM of the peak as black (empty pores) or white (filled pores).

In the images of the compacts with a low porosity (i.e. values approaching 0%) it could be seen that the resin had not penetrated the pores of the compacts. Therefore, the local porosity in these compacts was calculated as the percentage of black pixels only. In the compacts with the intermediate porosity (approx. 13%) and high porosity (approx. 22%), the resin had penetrated the pores, at least partly. Therefore, the local porosity in these compacts was calculated as the percentage black and white pixels of the total number of pixels in the image.

The principle of the quotient of the number of transitions (Q) was described earlier (21). In the present research we made use of the same principle. However, the number of transitions was calculated in the filtered gray-scale image. By doing so, the pores with a higher contrast between the pore and the grain are more important for the calculation of Q than the pores with only a small contrast between the pore and the grain. This method was chosen since it was believed that pores with a higher contrast between the pore phase and the grains, were deeper pores i.e. larger in the third dimension and are considered to have a more pronounced effect on the mechanical strength. The number of transitions was calculated as the sum of the (absolute) change in pixels value between all adjacent pixels in one direction (either y and x or z and x). The quotient number of transitions was then calculated according to the following equations. For the plan images:

$$Q_P = \frac{N_{Ty}}{N_{Tx}} \quad (1)$$

And for the elevation images:

$$Q_E = \frac{N_{Tz}}{N_{Tx}} \quad (2)$$

In which:

Nomenclature

Q_P or Q_E	quotient of the number of transitions in [Plan or Elevation] image(s)
N_{Ty}	sum of the absolute change in pixel value between all adjacent pixels in the y-direction
N_{Tx}	sum of the absolute change in pixel value between all adjacent pixels in the x-direction
N_{Tz}	sum of the absolute change in pixel value between all adjacent pixels in the z-direction

RESULTS AND DISCUSSION

Mechanical Strength

Figure 2 shows some force–displacement curves of the crushing of starch cubes with different porosities. Some images of the fractured cubes are also shown to illustrate the result of the different behaviour during fracture. The upper part of Fig. 2 shows the curves for crushing in the *x*-direction and the lower part of Fig. 2 shows the crushing in the *z*-direction. Arrows indicate the points defined as yield point (the first maximum or the intersection of the regression lines of the first and the second linear part of the curve) whereas the points where fracture occurred are indicated with an "*x*". The shapes of the curves change dependent on the porosity. With increasing porosity, the yield point becomes less and less pronounced and fracture occurs at lower forces. Figure 3 shows the crushing force and the yield strength in the *x*-direction and the *z*-direction at different porosities. The crushing force decreases with increasing porosity. However, at all porosities the crushing force was higher when the tablets were crushed in the *z*-direction. For both directions the relation between crushing force (F) and porosity (ε) showed an exponential relation with an R-squared value of 0.99 ($F = 5176.e^{-0.063\varepsilon}$ for the crushing force in the *z*-direction and $F = 2854.e^{-0.058\varepsilon}$ for the crushing force in the *x*-direction).

The yield strength of the specimen also decreases with increasing porosity. At porosities below 10% there is no difference in the yield strength measured in the *x*- or *z*-direction as can be seen in Fig. 3. However, at porosities higher than 10%, the yield strengths start to deviate from each other. This is indicated by a trend line of the values for the yield strength of compacts with a porosity higher than 10%. The equation for the trend line for the yield strength in the *z*-direction (yield strength$_z = -37.1\varepsilon + 1851$ [$R^2 = 0.925$]) is different from the one describing the yield strength in the *x*-direction, (yield strength$_x = -57.5\varepsilon + 2014$ [$R^2 = 0.973$]). The 95% confidence intervals of the intercept of the trend lines show some overlap, but this is not the case for the 95% confidence interval of the slope of the lines. Below a certain porosity the compacts do not break anymore, but only yield.

Image Analysis

Figure 4 shows some original plan and elevation images from compacts with low, intermediate and high porosity. All images are taken from the 0 mm plane. Pores that are filled with resin are white, unfilled pores are black, and the starch grains have an intermediate gray intensity. Resin has not penetrated all the pores, especially in the compacts with the lowest porosity. The local porosity determined with image analysis was slightly higher than the porosity

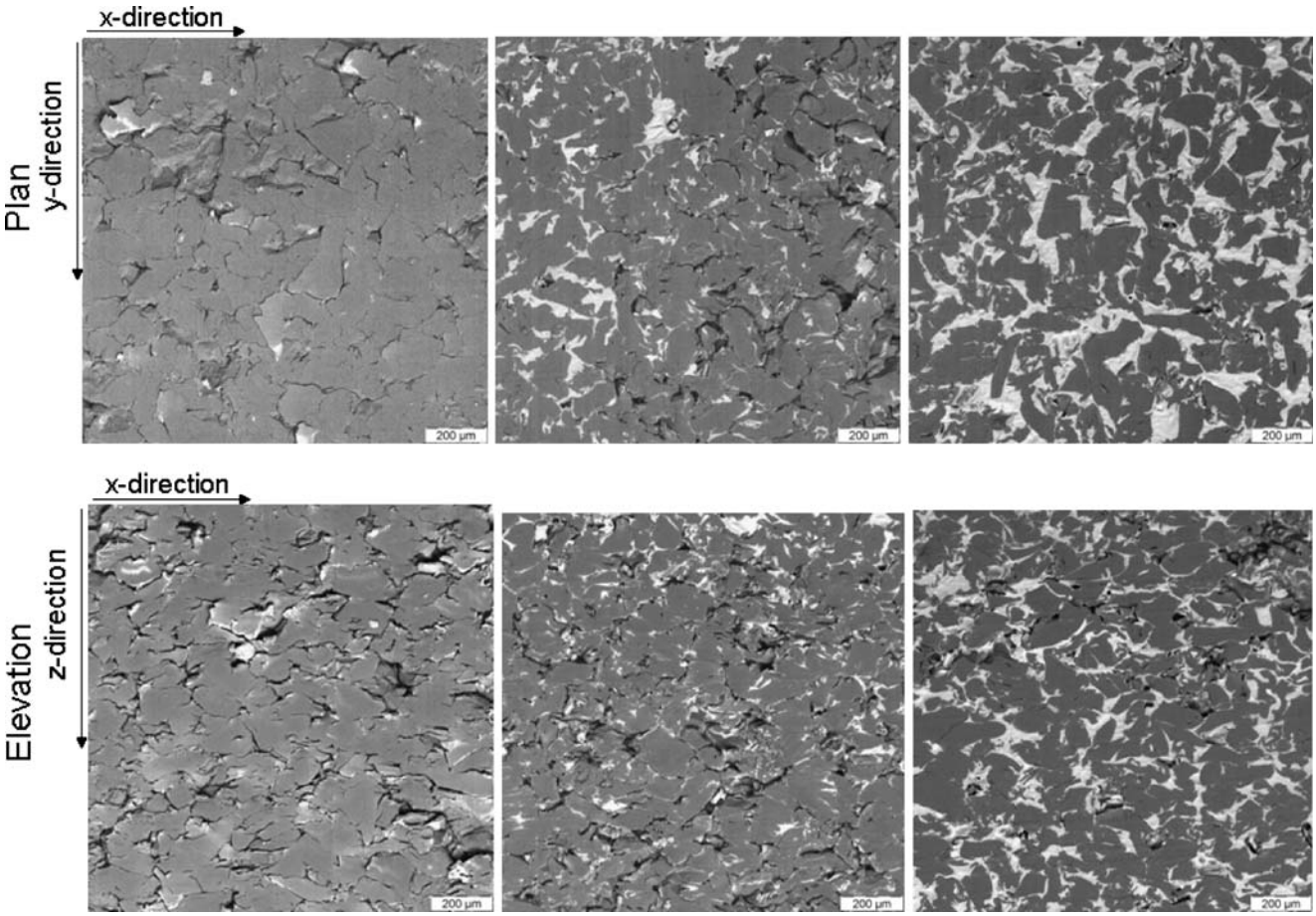

Fig. 4. Original plan and elevation images of starch cubes with a porosity of 0% (*left*), 13% (*middle*), and 24% (*right*). All images are taken from the 0 mm plane

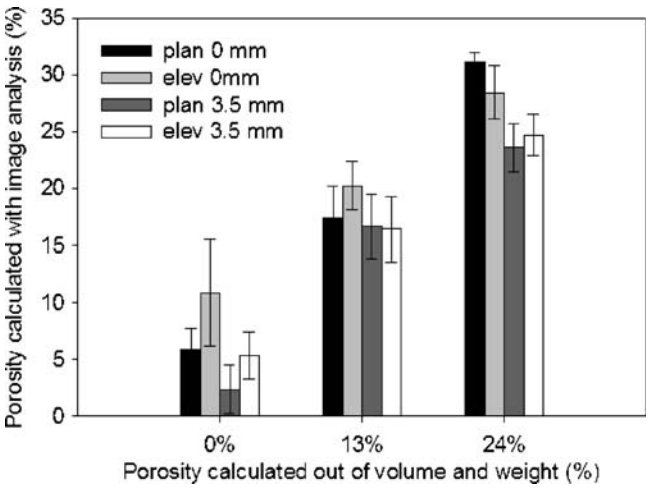

Fig. 5. Local porosity as calculated with image analysis in the images taken from 0 mm from the side and from images taken from 3.5 mm from the side

determined out of weight and volume (Fig. 5). Due to a lower surface roughness on the 3.5 mm plane, the local porosity was lower than at the 0 mm plane (note that the 3.5 mm plane was made visible by removal of material and subsequently polished, whereas for the 0 mm plane only the microtome was used). Tablets with a porosity of 0% as calculated out of volume and weight of the tablet were not completely transparent indicating that the actual porosity was not zero. This is in agreement with the results found with image analysis that also indicate that the porosity of the densest compacts is somewhat above 0%.

It can also be seen in Fig. 4 that there is no orientation in the plan images, while the pores in the elevation images seem to be mainly oriented along the *x*-direction. For the plan images no preferential direction of the pores was expected since the direction in which the image was taken was the same as the direction of compression. Visual inspection of the images confirmed that there was no preferential direction of the pores. This would mean that the quotient of transitions equals unity. However, this is not the case as can be seen in Fig. 6 which shows the quotient number of transitions for the plan and the elevation images. This can be caused by the fact that the images are taken with a scanning electron microscope. The transitions in the scanning direction could be less sharp than the transitions perpendicular to this direction. This could mean that even in images of an isotropic structure a quotient of transitions lower than unity is found.

There is a significant difference in the quotient of transitions between the plan and the elevation images ($p < 0.01$, Mann–Whitney test, SPSS 12.0.1). This applies to all porosities and at both locations in the tablet except for 0% at the 3.5 mm plane (from this plane, only three elevation images could be used because of technical problems with the other six images). A higher quotient in the elevation images than in the plan images means that the elevation images have relatively more transitions in the *z*-direction (see Eqs. 1 and 2). This means that the pores are preferentially oriented in the *x*-direction (perpendicular to the direction of compression) which can also be seen with the naked eye in the images in Fig. 4.

Pore Direction

The observation that the pores are mainly oriented in the *x*-direction is probably caused by the combination of particle deformation and stress relaxation. Pregelatinized starch is a ductile material which shows visco-elastic deformation during compaction and always some elastic recovery afterwards (24). The high moisture (16.7%) content facilitates deformation of the material (25,26). This deformation behaviour combined with uni-axial compression will result in pancake like shaped particles. When the decompression speed is extremely low (0.001 kN/s), the compact shows only a minor porosity expansion. This can be deducted from the increase in compact thickness calculated out of the thickness immediately after compression and after 24 h (0.9% sd. 0.2%). After this small expansion the pancake like stacking stays intact. In images of tablets with a low porosity a large number of transitions in the *z*-direction (direction of compression) can therefore be seen, corresponding to a large difference in quotient of transitions between the plan and the elevation images. For the compacts with higher porosities, having been subjected to a faster decompression rate, the increase in compact thickness is 2.8% sd. 0.4%. The structure is less dense, resulting in a lower number of transitions in the *z*-direction and consequently a smaller difference in quotient of transitions between the plan and the elevation images.

Crushing Force

When a body containing fine cracks is subjected to compressive stress, the fine cracks extend parallel to the

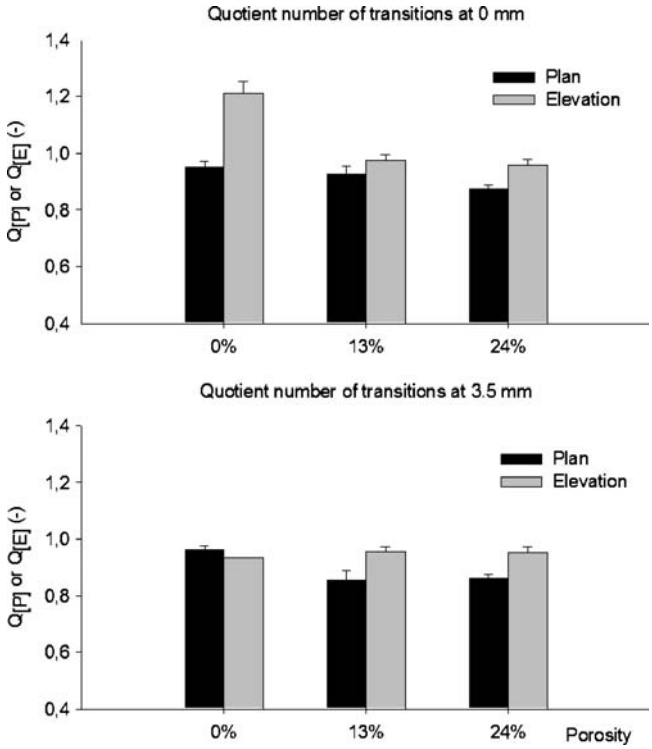

Fig. 6. Quotient of the number of transitions in the plan and elevation images of the compacts of low, intermediate, and high porosity from the plane at 0 mm from the side of the cube (*above*) and from the plane at 3.5 mm from the side (*below*)

compression axis causing failure planes parallel to the compressive stress (27). If the cracks are slightly off with respect to the direction of the applied load, wing cracks appear along the loading direction, splitting the material into slender columns which then fail (27,28). It is therefore not difficult to imagine that the larger the dimensions of the cracks along the compaction direction, the lower the crushing force will be when crushed in compression. This is why the crushing force of the starch cubes in the *x*-direction is much lower than the crushing force in the *z*-direction (see Fig. 3). Apparently, the pores in the cubes (which are mainly oriented in the *x*-direction) act as some sort of quasi cracks.

Another observation supporting this hypothesis is that the fracture of the starch cubes when crushed in the *x*-direction showed failure planes parallel to the compressive stress especially at the highest porosity (see Fig. 2). These are probably caused by the opening of the pores in the *x*-direction. When the cubes were crushed in the *z*-direction the fragments of the cube after fracture more looked like slender columns after failure (Fig. 2). This could indicate wing crack development during crushing in the *z*-direction.

Porosity is a property without direction. This paper shows that direction of pore structure plays a significant role as can be deducted from Fig. 3 where it is shown that at a similar porosity the crushing force in the *x*-direction is significantly different from that in the *z*-direction (7–17). Formulation approaches that minimize the anisotropy in pore structure, possibly by reducing wall effects by focussing on lubrication, will help to control this effect.

Yield Strength

There was no difference in yield strength between the *x*-direction and the *z*-direction of the cube at porosities lower than 10%. Furthermore, there was no difference in porosity measured in the plan images and in the elevation images (Fig. 5). Since yielding is a material property, yielding does not depend on the direction of the pores, but on the pore fraction (porosity) in the cross section. Because the porosity in the plan images is similar to the porosity measured in the elevation images, it is not surprising that there was no difference in yield strength between the *x*-direction and the *z*-direction. The explanation for the observation that the yield strength decreases with increasing porosity is the same. With increasing porosity, the cube consists of less material resulting in a lower yield strength of the cube.

At porosities higher than 10% the values for the yield strength in the *x*-direction and *z*-direction deviate more from each other, but it is questionable whether at these high porosities a yield strength is present at all, because the fracture shows more brittle behaviour with increasing porosity. In case of brittle fracture no plastic deformation takes place and thus no yielding point can be defined.

CONCLUSION

The anisotropy in pore structure in a cubic starch compact could be detected with image analysis. The different compressive forces at which fracture occurred in the *x*-direction and in the *z*-direction could be explained with these results. The yield strength of the cube was not dependent on the pore direction at porosities lower than 10%, showing that the pore direction influences the force at which fracture occurs, but does not influence the yield strength of the compact.

REFERENCES

1. K. van der Voort Maarschalk, and G. K. Bolhuis. Improving properties of materials for direct compression. *Pharm. Technol.* **23**:34–38 (1999).
2. B. Johansson, M. Wikberg, R. Ek, and G. Alderborn. Compression behaviour and compactability of microcrystalline cellulose pellets in relationship to their pore structure and mechanical properties. *Int. J. Pharm.* **117**:57–73 (1995).
3. M. Eriksson and G. Alderborn. The effect of original particle size and tablet porosity on the increase in tensile strength during storage of sodium chloride tablets in a dry atmosphere. *Int. J. Pharm.* **113**:199–207 (1995).
4. R. W. Rice. Relation of tensile strength–porosity effects in ceramics to porosity dependence of Young's modulus and fracture energy, porosity character and grain size. *Mat. Sci. Eng. A-Struct* **A112**:215–224 (1989).
5. E. Ryshkewitch. Compression strength of porous sintered alumina and zirconia. *J. Am. Ceram. Soc.* **36**:65–68 (1953).
6. W. H. Duckworth. Discussion of Ryshkewitch paper by Winston Duckworth. *J. Am. Ceram. Soc.* **36**:68 (1953).
7. J. M. Newton, G. Alderborn, and C. Nyström. A method of evaluating the mechanical characteristics of powders from the determination of the strength of compacts. *Powder Technol.* **72**:97–99 (1992).
8. G. Alderborn and C. Nyström. Studies on direct compression of tablets IV. The effect of particle size on the mechanical strength of tablets. *Acta Pharm. Suec.* **19**:381–390 (1982).
9. T. Ando, H. Yuasa, Y. Kanaya, and K. Asahina. Studies on anisotropy of compressed powder III. Effects of different granulation methods on anisotropy, pore size and crushing strength of tablets. *Chem. Pharm. Bull.* **31**:2045–2054 (1983).
10. G. Alderborn and C. Nyström. Radial and axial tensile strength and strength variability of paracetamol tablets. *Acta Pharm. Suec.* **2**:1–8 (1984).
11. S. Malamataris, T. Hatjichristos, and J. E. Rees. Apparent compressive elastic modulus and strengths isotropy of compacts formed from binary powder mixes. *Int. J. Pharm.* **141**:101–108 (1996).
12. C. Nyström, K. Malmquist, and J. Mazur. Measurement of axial and radial tensile strength of tablets and their relation to capping. *Acta Pharm. Suec.* **15**:226–232 (1978).
13. J. M. Newton, G. Alderborn, C. Nyström, and P. Stanley. The compressive to tensile strength ratio of pharmaceutical compacts. *Int. J. Pharm.* **93**:249–251 (1993).
14. K. Kachrimanis and S. Malamataris. Compact size and mechanical strength of pharmaceutical diluents. *Eur. J. Pharm. Sci.* **24**:169–177 (2005).
15. G. Alderborn, E. Borjesson, M. Glazer, and C. Nyström. Studies on direct compression of tablets XIX. The effect of particle size and shape on the mechanical strength of sodium bicarbonate tablets. *Acta Pharm. Suec.* **25**:31–40 (1988).
16. S. Galen and A. Zavaliangos. Strength anisotropy in cold compacted ductile and brittle powders. *Acta Mater.* **53**:4801–4815 (2005).
17. M. P. Mullarney and B. C. Hancock. Mechanical property anisotropy of pharmaceutical excipient compacts. *Int. J. Pharm.* **314**:9–14 (2006).
18. J. T. Fell and J. M. Newton. Determination of tablet strength by the diametral-compression test. *J. Pharm. Sci.* **59**:688–691 (1970).
19. E. H. Andrews. Fracture phenomena in polymers I. In E. H. Andrews (ed.), *Fracture in polymers*, Oliver and Boyd, Edinburgh, 1968, pp. 37–73.
20. I. M. Ward. Review: the yield behaviour of polymers. *J. Mater. Sci.* **6**:1397–1417 (1971).
21. Y. S. Wu, H. W. Frijlink, L. J. van Vliet, I. Stokroos, and K. van der Voort Maarschalk. Location dependent analysis of porosity and pore direction in tablets. *Pharm. Res.* **22**:1399–1405 (2005).
22. http://www.diplib.org. (accessed 7/1/07).

23. T. Q. Pham, and L. J. van Vliet. Separable bilateral filtering for fast video preprocessing. in Proc. IEEE Int. Conf. on Multimedia & Expo. 2005. Amsterdam.
24. K. van der Voort Maarschalk, H. Vromans, G. K. Bolhuis, and C. F. Lerk. The effect of viscoelasticity and tabletting speed on consolidation and relaxation of a viscoelastic material. *Eur. J. Pharm. Biopharm.* **42**:49–55 (1996).
25. J. E. Rees and K. D. Tsardaka. Some effects of moisture on the viscoelastic behaviour of modified starch during powder compaction. *Eur. J. Pharm. Biopharm.* **40**:193–197 (1994).
26. K. van der Voort Maarschalk, H. Vromans, W. Groenendijk, G. K. Bolhuis, and C. F. Lerk. Effect of water on deformation and bonding of pregelatinized starch compacts. *Eur. J. Pharm. Biopharm.* **44**:253–260 (1997).
27. M. F. Ashby and S. D. Hallam. The failure of brittle solids containing small cracks under compressive stress states. *Acta Metall.* **34**:497–510 (1986).
28. C. E. Renshaw and E. M. Schulson. Universal behaviour in compressive failure of brittle materials. *Nature* **412**:897–900 (2001).